Monitoring the risk of large building collapse using persistent scatterer interferometry and GIS

Sang-Wan Kim[1], Jung-Hyun Choi[2], Sang-Hoon Hong[3], Ju-Hyung Lee[4], Jinwoo Cho[4], and Moung-Jin Lee[5, *]

[1] *Department of Geoinformation Engineering, Sejong University, Seoul, Korea*
[2] *Department of Earth System Sciences, Yonsei University, Seoul, Korea*
[3] *Department of Geological Sciences, Pusan National University, Busan, Korea*
[4] *Geotechnical Engineering Research Division, Korea Institute of Civil Engineering and Building Technology, Gyeonggi-do, Korea*
[5] *Environmental Assessment Group/Center for Environmental Assessment Monitoring, Korea Environment Institute (KEI), Sejong-si, Korea*

ABSTRACT

In this study, we analyzed the displacement of large buildings in downtown areas. First, we improved an existing Persistent Scatterer InSAR technique and developed an algorithm to calibrate temperature data. Second, we collated TerraSAR-X satellite images of Seoul captured over 22 months from November 2011 to September 2013, automatic weather system data, and a topographic map. Third, the Gangnam Station area, one of the most crowded areas of downtown Seoul, was selected as a study area for precise analysis. We used the algorithm to analyze the displacement rates of downtown buildings. Fourth, by processing GIS data of the study area, we analyzed the individual displacements of 15 large buildings. These buildings occupied the top 0.1 percent of the building area. The average displacement rate of these 15 large buildings caused by vertical land rising and settlement was 4.7 mm. Fifth, three of the 15 large buildings were found to have undergone significant settlement ('-' displacement). One of them, CHA Gangnam Medical Center, which is located at one of the exits of Eonju Station. Over the study period, a maximum displacement of -20 mm was observed. In addition, these buildings were located near subway lines and very close to areas where road collapses and underground holes had been reported in the past. These results show that the method used in this study is effective for analyzing the displacement of large buildings in broad downtown areas. Using this method, it will be possible to respond to signs of settlement and collapse of large buildings in advance.

1. INTRODUCTION

Rapid economic growth and urbanization have become the main causes of the unplanned development of urban underground spaces (UN 2014). In particular, around 1036 land subsidence events were reported in Seoul, South Korea, in 2015, including a case where walls in eight houses cracked and collapsed during excavation work for a new building in Nokbeon-dong, Eunpyeong-gu, Seoul (KICT 2015). Land subsidence is a type of disaster that causes significant economic damage and loss of life. It occurs mostly in landfills developed on soft ground, abandoned mines, and groundwater exploitation sites. Recently, however, land subsidence events have been frequently reported in downtown areas where large structures and underground facilities are concentrated. Such damage is widespread, and it is highly likely to result in secondary and tertiary tragedies such as the collapse of large buildings. In addition, land subsidence in downtown areas is a direct cause of signs of abnormal building movement on the ground. It has become more important to monitor and predict the time and range of signs of abnormal movement in large buildings in downtown areas. These events are often caused by building extensions and

_____

* *Corresponding author*
  E-mail: leemj@kei.re.kr

integration with underground utilities. By monitoring these events, it is possible to manage the safety of large buildings preemptively and minimize the potential economic damage and loss of life.

Abnormal building movements have been monitored so far by installing equipment such as settlement extensometers directly into their structures. This enables us to observe long- and short-term changes. However, this method is costly, and only the displacement of selected buildings can be measured. Thus, it is not suitable for monitoring and managing the safety of broad downtown areas.

Recently, a synthetic aperture radar (SAR), which uses satellite radar images, has been widely used to acquire images regularly regardless of the time of day or weather conditions (Massonnet and Feigl 1998). This technology is recognized as being highly suited to monitoring abnormal events in downtown areas (Zebker et al. 1994). In particular, SAR satellites such as TerraSAR-X (TSX), COSMO-SkyMed (CSK), and KOMPSAR 5 have very high resolution and short revisit times (TSX: 11-day, CSK: approx. 4-day), offering high-quality spatio-temporal images with precisions similar to those obtained from ground observations. In addition, persistent scatterers SAR interferometry (PSInSAR) has been recognized as a suitable technology for systematically monitoring the displacement of structures for safety management. This technology offers high theoretical precision, to the level of mm yr^{-1} or lower under the assumption of an ideal scatterer and linear displacement. Ferretti et al. (2007) showed sub-millimeter accuracy in an experiment based on dibedral reflectors. Crosetto et al. (2007) reported standard deviations of the velocities ranging from 0.45 - 0.66 mm yr^{-1}. Using this technology, we can observe time-series displacements using persistent scatterers (PS) technology (Ferretti et al. 2001; Colesanti et al. 2003; Adam et al. 2009). When satellite images observed using this technology are used for calculating the ground movements of artificial structures in downtown areas, we obtain a very high precision (mm yr^{-1}), close to the theoretical precision level (Crosetto et al. 2015).

There are only a few cases where PS method has been utilized to analyze the displacements of large buildings in downtown areas. Among the time-series analysis techniques based on multi-temporal SAR images, PS method has been widely used to analyze ground displacements in downtown areas. For instance, Ferretti et al. (2000) analyzed the amount of settlement observed over 7 years in downtown Pomona, California, using European Remote Sensing (ERS). Other studies have been performed using PSInSAR, including a study on ground displacements caused by landslides and tectonic movements (Colesanti et al. 2003); a study on the ground displacement of abandoned mines observed using L-band JERS-1 radar images (Jung et al. 2007); and a study on the ground displacement of reclaimed coastal areas (Kim et al. 2010). Recently, 1-m-level high-resolution SAR images

have been used for precise observation of the displacements of individual artificial structures in downtown areas (Reale et al. 2011; Bonano et al. 2013; Fornaro et al. 2013; Kim et al. 2013). Bakon et al. (2014) used high-resolution TerraSAR-X images to observe the displacement of Gabcikovo Dam, which is located in Slovakia, with a precision of 2 mm yr^{-1}, and also used PS technology to observe the settlement of buildings around construction sites in downtown areas in Slovakia. Karila et al. (2013) calculated the settlement of the official residence of Turku City Hall in Finland. Their result was very similar to the actually observed data. Hence, their study proved that PSInSAR is a practical method for observing the displacement of large structures. However, only specific buildings were targeted in these earlier studies.

Against this backdrop, this study aimed to use PS method and GIS to monitor the displacement of multiple buildings in downtown areas, rather than a single building. To do so, first, a PS-based displacement analysis algorithm was applied to the study area. We used this to analyze the displacement of multiple downtown buildings. Second, the displacements of the 0.1% of largest buildings were calculated individually with the aid of GIS. Third, the relative displacement of the large buildings in the study area was analyzed. Those with high displacement rates were selected for precise analysis. We focused on precisely analyzing the relative displacement of large downtown buildings rather than on the displacement of a particular building. Using this approach, the displacement of large buildings can be effectively monitored in advance, helping to prevent potential damage.

2. STUDY AREA

We selected the Gangnam Station area in Seoul in the pilot study to assess the PS method to monitoring abnormal building movement in downtown areas. Seoul is geopolitically located in the middle of the Korean Peninsula, and the Han River flows horizontally across Seoul (Fig. 1). The Gangnam Station area is the most crowded area in Seoul, with a daily floating population of 200000. Five subway lines pass near the Gangnam Station area.

A relatively thick alluvium is developed in the study area, and it has been reported that groundwater leakage caused by large-scale civil works such as construction of subways and large structures is serious (Seoul Metropolitan Government 2014). The subsurface alluvial layer may be lost to groundwater, consequently the ground may be formed to collapse. It is believed that the road collapses occurring in Seoul is due to this cause (Seoul Metropolitan Government 2014).

Road collapses are frequently reported in Seoul. To respond to such events, Seoul Metropolitan Government conducted an investigation jointly with GEO Search, a Japanese company specialized in detecting underground holes. Overall, 41 empty holes were detected in 4 downtown areas, with
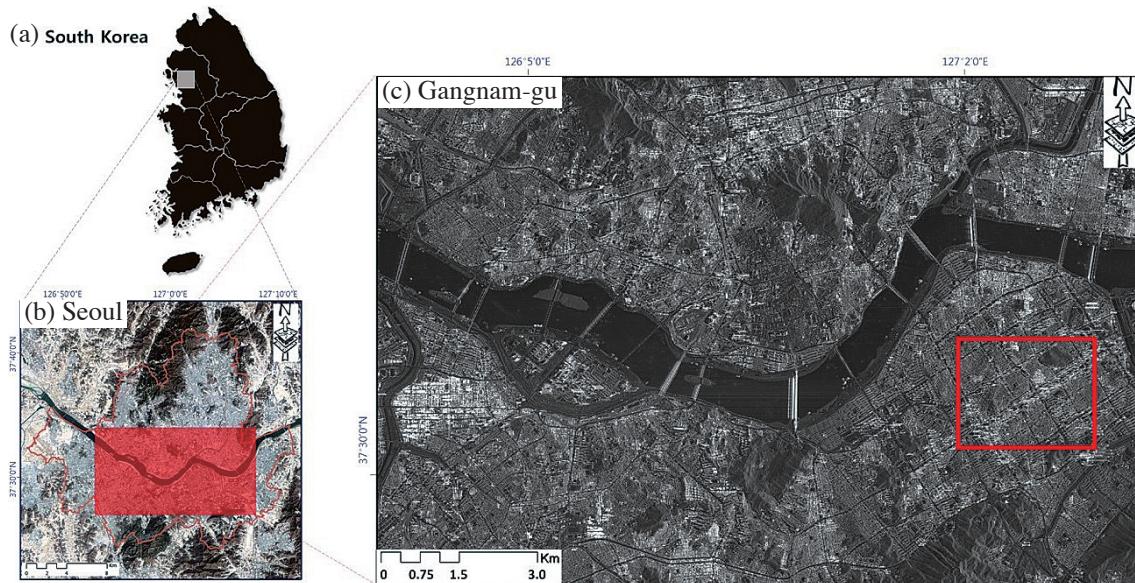
Fig. 1. Location of Study Area. (a) Map of South Korea, (b) The capital city of South Korea, Seoul metropolitan city, (c) TerraSAR-X image of Seoul city (Red box: area of interest corresponding to Figs. 4 and 5).

a total length of 61.3 km (Seoul Metropolitan Government 2014). The Gangnam Station area, one of the study areas in the investigation, covered 32 km (approx. 50% out of total investigation length), and 18 underground holes were detected underneath this area. A lot of people commute to and from the Gangnam Station area, and five subway lines pass through the area. Construction projects for new buildings or the expansion of existing buildings are frequently carried out there.

Land subsidence and construction sites in Seoul directly affect the displacement of large buildings on the ground, increasing the risk of collapse. In addition, in the past, land subsidence was only studied in areas where land subsidence events had already been observed. Thus, it was impossible to monitor the middle phase of the displacement of large structures. Against this backdrop, we analyzed the displacement of large buildings in the study area using PS analysis.

3. DATA

High-resolution satellite images with short revisit times can be used to monitor the displacement of large buildings in downtown areas. In other words, satellites with short-frequency bands normally have high spatial resolution and thus the shorter the observation time, the more effectively we can observe the displacements that occur in a short period of time. There is a wide range of data collected by currently operating satellites. We used satellite images acquired by TerraSAR-X, which has a high resolution and a short revisit time, in this study.

TerraSAR-X is a radar satellite operated by the German Aerospace Center (DLR). It was launched on 15 June

2007. The satellite circles the Earth every 11 days in a polar orbit at an altitude between 512 and 530 km. Its center frequency is 9.65 GHz in the X-band (http://www.dlr.de). We used the Strip Map mode, which has a resolution of 3 m. Each image covered an area of 30 km × 50 km.

We combined three types of data in this study. First, we used the data from the TerraSAR-X, as discussed above. A total of 47 images of Seoul were used. These images were captured over 22 months from November 2011 to September 2013 (Fig. 2). Out of the 47 satellite images, we selected the one captured on 13 April 2012, as the master image, and the 46 interference pairs were generated and analyzed. Figure 2 shows the baseline distance between the 46 interference pairs used in the analysis. Second, the automatic weather system (AWS) used in Gangnam-gu was used to eliminate the effect of thermal expansion. The temperature on the days the images were acquired are collected from the AWS, which is shown in Table 1. Third, we acquired a topographic map with a scale of 1:5000. This map was provided by the National Geographic Information Institute (NGII). We used this to extract spatial information relating to large buildings in the study area.

4. METHOD

4.1 Displacement Measurements

We applied a technique based on persistent scatterers to make precise observations of displacement events at each building in the downtown area, where there are many high-rise buildings. Differential interferometric phases (ϕ) of persistent scatterer candidates (PSC) were identified at large buildings in SAR images. Next, we included the following
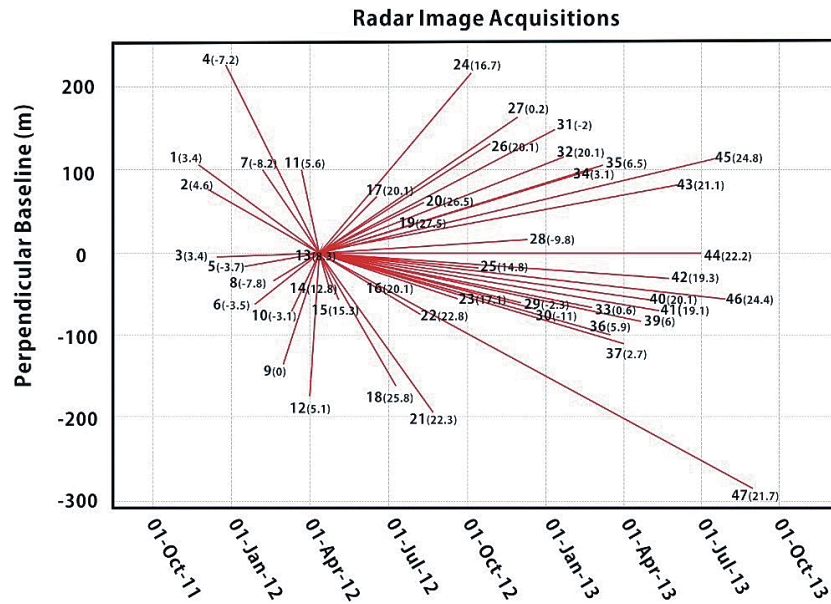
Fig. 2. Baseline plot for PS analysis with temperature at each acquisition (text next to dot). The dots and lines represent TerraSAR-X images and interferometric pairs.

Table 1. Temperature of SAR image observation day from AWS, refined temperature by PS processing, and thermal expansion displacement.

Date	Temperature (°C)		Thermal expansion displacement* (cm)	Date	Temperature (°C)		Thermal expansion displacement* (cm)
	AWS	Refined by PS processing			AWS	Refined by PS processing	
2011.11.22	3.6	5.6	-0.4	2012.10.17	12.0	11.9	0.3
2011.12.03	3.4	4.5	-0.6	2012.10.28	12.1	11.5	0.3
2011.12.14	-3.1	1.0	-1.0	2012.11.30	-0.8	-0.9	-1.2
2011.12.25	-6.3	-6.5	-1.8	2012.12.11	-4.8	-5.8	-1.8
2012.01.16	2.9	-0.3	-1.1	2012.12.22	-8.3	-4.0	-1.6
2012.01.27	-1.3	-3.0	-1.4	2013.01.02	-12.6	-9.5	-2.2
2012.02.07	-7.1	-6.7	-1.9	2013.01.13	-1.9	-4.8	-1.6
2012.02.18	-3.7	-4.2	-1.6	2013.01.24	-8.5	-4.4	-1.6
2012.02.29	8.6	3.0	-0.7	2013.02.15	-2.3	-3.1	-1.5
2012.03.11	-0.9	-0.8	-1.2	2013.02.26	3.7	1.0	-1.0
2012.03.22	5.3	5.0	-0.5	2013.03.09	1.5	2.9	-0.7
2012.04.02	5.4	7.2	-0.2	2013.03.20	1.8	1.9	-0.9
2012.04.13	11.1	9.3	0.0	2013.03.31	9.4	4.4	-0.6
2012.04.24	15.5	13.6	0.5	2013.04.11	7.0	4.6	-0.5
2012.05.05	18.3	16.7	0.9	2013.04.22	11.1	8.2	-0.1
2012.06.07	22.3	23.4	1.6	2013.05.03	13.7	11.9	0.3
2012.06.18	26.1	23.8	1.7	2013.05.14	19.5	18.9	1.1
2012.07.10	23.6	27.7	2.2	2013.05.25	23.8	21.2	1.4
2012.08.01	31.0	30.8	2.5	2013.06.05	24.9	22.4	1.5
2012.08.12	26.8	28.6	2.3	2013.06.27	25.2	25.9	1.9
2012.08.23	23.5	25.9	1.9	2013.07.19	27.1	28.1	2.2
2012.09.03	22.0	27.7	2.2	2013.07.30	26.4	30.2	2.4
2012.09.25	21.5	21.6	1.4	2013.09.01	22.8	26.5	2.0
2012.10.06	19.2	17.2	0.9				

*Note: * assuming a structure length of 100 m with respect to master image (2012.04.13).*

in our equation: a component caused by displacement that occurred during the observation period (ϕ_{defo}); a component caused by errors in the digital elevation model (DEM) used to eliminate the topographic effects ($\phi_{DEM\ error}$); a component caused by changes in the atmospheric conditions such as humidity, temperature, and pressure (ϕ_{APS}); and a component caused by building displacement due to thermal expansion ($\phi_{thermal}$), as well. The equation is as follows (Monserrat et al. 2011).

$$\phi = \phi_{defo} + \phi_{DEM\ error} + \phi_{APS} + \phi_{thermal} + \phi_{res} \tag{1}$$

Here, ϕ_{res} is the residual component, which was not modeled. The displacement caused by thermal expansion can be calculated using Eq. (2). We multiply the difference in the air temperature between the two images ($\Delta Temp$) by the thermal expansion coefficient (TEC) at each point and the length of a structure.

$$\phi_{thermal} = \frac{4\pi}{\lambda} \Delta Temp \cdot (TEC \cdot \Delta l) \tag{2}$$

The typical coefficient of linear thermal expansion of reinforced concrete structures is $11.7 \times 10^{-6}/°C$ (Merritt 1976). Thus, when the temperature difference is 50°C in a 100-m-tall building, approximately 6 cm of contraction or expansion occurs (Crosetto et al. 2015). Seoul, the area of focus in this study, is crowded with large structures. In addition, since the annual temperature difference in the city is as high as ±40°C, the displacement caused by the thermal expansion of buildings is over ±1 cm annually. Therefore, thermal expansion factors were taken into account in the model used for time-series analysis based on the PS method.

From Eq. (1), we first removed ϕ_{APS}, which was estimated using PSCs on the ground. Then the existing two-variable (DEM error, linear displacement) modeling algorithm was applied to calculate the DEM errors and linear displacement. Using the remaining phases, an algorithm to estimate phases caused by thermal expansion was applied (Wegmuller and Werner 2015). Air temperature data obtained by the AWS located at Seocho, which is located in the study area, on the days when each SAR satellite image was captured were collected. We were then able to use these data to correct all of the DEM errors, linear displacements, and thermal expansion factors (Fig. 3). The air temperature data used to model the thermal expansion displacement contain observational errors and regional temperature differences. Such errors are expressed in residual components. These remained as a proportion of the thermal expansion. Thus, when the residual components and the thermal expansion coefficient were highly linearly correlated, temperature values were optimized by repeating the data processing process (Fig. 3). Based on this process, the estimated minimum

and maximum calibrated temperature values were -5.6 and 5.7°C, respectively.

4.2 Spatial Analysis of the Displacement Rates of Large Buildings

The displacement of large buildings in the study area was analyzed by overlapping processed satellite radar image data and a topographic map with a scale of 1:5000. To do so, first, all of the office buildings, apartment buildings, and row houses were extracted from the map. Second, the early form of the extracted buildings was polylined, and the lines were rearranged to generate polygons. Third, the PS analysis results were matched with the coordinates on the map. Since the reference coordinate systems of radar satellite images and the topographic map were WGS (World Geodetic System) 84 and GRS 80 (Geodetic Reference System 1980), respectively, the two sets of data were standardized into GRS 80. Fourth, the displacement rates of individual large buildings were extracted. Out of the structures extracted from the map, large buildings were selected based on their surface-area-to-size ratio. The ratio applied here was selected to include the 0.1% of largest buildings. For instance, the total number of buildings in the Gangnam Station area is around 13185, and among them, those with a building area over 3500 m² (area ratio 0.1%) were categorized as large buildings. Based on this criterion, 15 buildings in the Gangnam Station area were selected as large buildings. The displacement rates of the individual selected large buildings were extracted.

5. RESULTS

5.1 Spatial Analysis of the Displacement Rates of Individual Large Buildings in the Study Area

TerraSAR-X amplitude images of the Gangnam Station area, including many high-rise buildings and two by-products of updated DEM and thermal expansion factors [$\frac{4\pi}{\lambda} \cdot TEC \cdot \Delta l$ in Eq. (2)] are presented in Fig. 4. Many skyscrapers are distributed in the research area, as seen in aerial photographs with 3D building model (Fig. 4b), but the DEM used as initial input data does not include information on the height of these buildings. From Fig. 4c, which shows the final DEM generated in the process of PS data processing, it can be confirmed that the heights of the high-rise buildings have been sufficiently corrected. The estimated factor of thermal expansion of most building structures is between -0.1 to 0.2 rad °C⁻¹ (Fig. 4d). Using the phase obtained by multiplying this factor by the temperature difference of each interferogram, we subtract the effect of thermal expansion of the building. The optimized temperatures and thermal expansion displacements with respect to reference image during PS analysis are presented in Table 1.

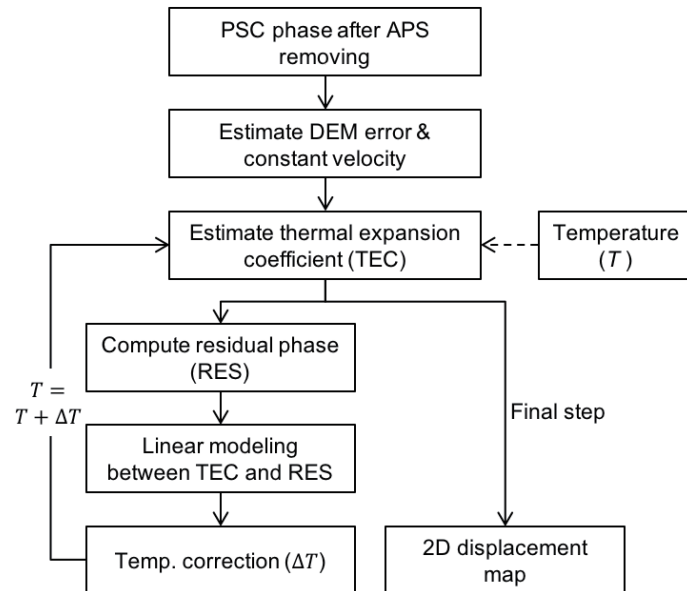Some structures show different factors of thermal

Fig. 3. Flow chart of the displacement estimation, including the temperature optimization.
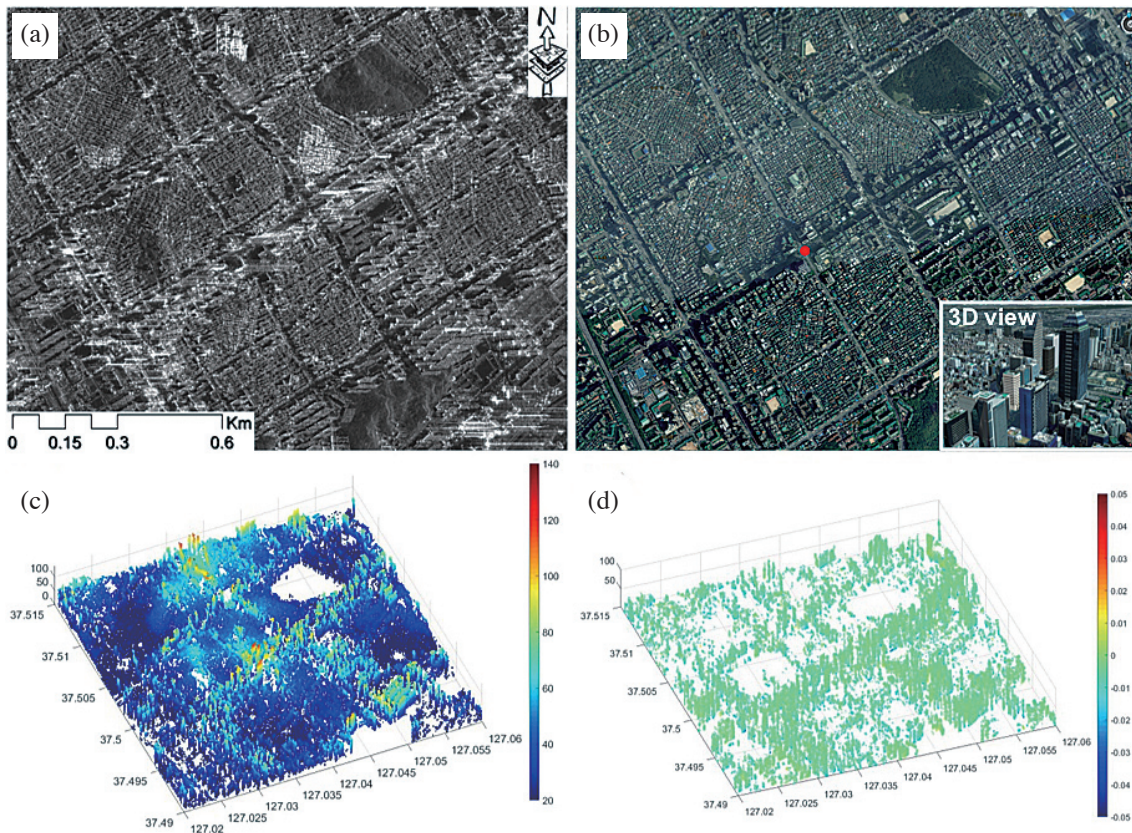

Fig. 4. (a) TerraSAR-X amplitude image, (b) aerial photograph with the inset showing 3D view of high-rise buildings around a red dot, (c) DEM with corrected building height, (d) thermal expansion factor estimated from PS analysis.

expansion, which is have been confirmed to be due to the differences in building materials. In the case of a steel structure, it is $12 \times 10^{-6}/°C$, which is different from the thermal expansion coefficient $11.7 \times 10^{-6}/°C$ of most reinforced concrete structures. Although we have no direct measurement data in our study area with which to verify the thermal expansion coefficient, we confirmed that the observation result was within a reasonable range compared to the thermal expansion coefficient presented in previous research reports (Crosetto et al. 2015).

To analyze the displacement rate of each large building spatially, the PS data were converted into GIS Point data, as shown in Fig. 5. The LOS displacement rates in Fig. 5 are marked with a color spectrum of yellow, green, and red by each PS point. No regional displacements were reported in the study area, so we selected a point with the highest temporal coherence in a stable ground area as the reference point. A stable ground area was defined from several long-term interferograms with small baselines, showing long-term displacement. The stable areas where very small displacement occurred during the study period, that is, those close to a "0" displacement rate, are colored green. Negative values, which indicate vertical subsidence, are colored yellow and those with a vertically raised surface are colored red.

Large buildings in the study area were extracted from a topographic map with a scale of 1:5000, and 15 of the largest buildings were selected. The largest building in the study area was the COEX Trade Center (72886.17 m²). This building had around 3900 PSInSAR points, which are displacement points. The displacement rates of the 15 selected buildings were analyzed, as shown in Table 2. Using the building polygons from GIS data, the PSs included in each building were extracted and the statistical values of the displacement values were obtained. There were two types of displacement observed in these buildings: those that have small average displacement and variation (COEX Trade Center, Gangnam Severance Hospital, etc.); those that have settlements only. In terms of large settlement, CHA Gangnam Medical Center, had the highest displacement rate (-7.1 mm yr⁻¹), followed by the Yeoksam Seohae The Blue Apartment (-5.4 mm yr⁻¹), and the Mercure Seoul Ambassador Gangnam Sodowe Hotel (-4.5 mm yr⁻¹). These results obtained using PS analysis can be used to extract, organize, and manage the displacement rates of individual large buildings or other structures that need to be analyzed.

5.2 Precise Analysis of the Displacement Rates of the Settlement of Buildings

In the study area, three large buildings that were found to have settled were analyzed precisely. The selected buildings, shown in Table 2, include No. 13 (Yeoksam Seohae, The Blue Apartment), No. 14 (Mercure Seoul Ambassador Gangnam Sodowe Hotel), and No. 15 (CHA Gang-nam Medical Center), which are marked as A, B, and C in Fig. 5. Three buildings with large displacements were extracted and analyzed from the results of large-scale structural displacement analysis in Gangnam Station area. Time series profiles of three selected buildings between November 2011 and September 2013 are presented in Fig. 6, showing the displacement of each PS and its evolution over time. Dots and bars indicate mean displacement and standard error estimated from standard deviation of neighboring PSs, respectively. The standard error can be interpreted as variation in the displacement of neighboring PSs or as measurement noise. The overall accuracy of each observation is within about 1 mm. The continuous line indicates the best-fit linear model (that is, constant velocity). The negative slope for the regression line indicates the subsidence at the scatterer.

Point A is located between Gangnam Station subway line 2 and Yangjae Station subway line 3. Figure 6a shows the time series displacement at Yeoksam Seohae, The Blue Apartment. The apartment building is a 10-story mixed-use building, into which people started to move in August 2012. Although some points that seem to be noise were included at the end of the observational period, displacements as high as -15 mm were observed during the study period. Point B is located between Yeosam Station subway line 2 and Eonju Station subway line 9. Over the study period, the Mercure Seoul Ambassador Gangnam Sodowe Hotel had the maximum displacement of -10 mm, as shown in Fig. 6b. The hotel was opened in March 2012. This displacement rate can be attributed to the completion of the construction and opening of the hotel. In addition, Eonju Station was within the investigation area mentioned above, in which underground holes were detected. Figure 6c shows the observed displacement graph of the CHA Gangnam Medical Center, which is located at one of the exits of Eonju Station. Over the study period, a maximum displacement of -20 mm was observed.

Unfortunately, no in-situ observations were made during the observation period of the TerraSAR-X satellite. We collected a proportion of the GPR (Ground Penetrate Radar) exploration results for underground cavity monitoring in 2014, although the observation period was inconsistent. In comparison with the partially released GPR exploration data, partial sagging of the lower strata was found in several major displacement areas, as observed by the satellite.

6. DISCUSSION AND CONCLUSION

Some large buildings were displaced, that is, vertical settlement was observed in the study area. Fifteen large buildings sized between 718 and 72886 m² were selected for analysis. The average displacement rate of these 15 large buildings caused by vertical land rising and settlement was 4.7 mm. The Mercure Seoul Ambassador Gangnam Sodowe Hotel, near the Yeoksam Station, and the CHA Gangnam Medical Center had settlements of -20 mm. A road collapse

Fig. 5. Geocoded LOS displacement map of PSs with high coherence (> 0.8) around the Gangnam Station area. Red dots indicate the displacement less than -3 mm yr^{-1}. Three large buildings with significant displacement are marked by A, B, and C.

Table 2. Statistics of displacement rates of large buildings (top 0.1% of the surface area to size ratios) in the study area.

| No.	Building Name	Area (m²)	No. of PS	Average displacement (mm)	Std. Dev. of displacement (mm)
1	COEX Trade Center	72886.17	3613	1.2	0.7
2	Gangnam Severance Hospital	10703.79	1194	0.3	0.7
3	Posco Center	7371.19	305	1.5	0.8
4	Samsung Electronics Seocho Building	6549.48	496	-0.2	1.2
5	Sporworld Building	5316.17	554	1.5	0.6
6	Renaissance Hotel	5099.28	392	0.8	0.5
7	Korea City Air Terminal	5002.29	304	1.6	0.7
8	Hansol Pilriah Shopping Center	4417.19	500	0.7	0.7
9	Grand Intercontinental Seoul Parnas	4416.89	58	1.6	0.8
10	Choonghyun Church	4037.71	289	0.7	0.4
11	Sookmyung Girls Middle/High Schools	3880.61	164	-0.6	0.7
12	Lotte Department Store Gangnam	3798.74	715	0.2	0.6
13	Yeoksam Seohae, The Blue Apartment	1475.99	85	-5.4	3.0
14	Mercure Seoul Ambassador Gangnam Sodowe Hotel	739.54	144	-4.5	1.7
15	CHA Gangnam Medical Center	718.27	76	-7.1	3.7
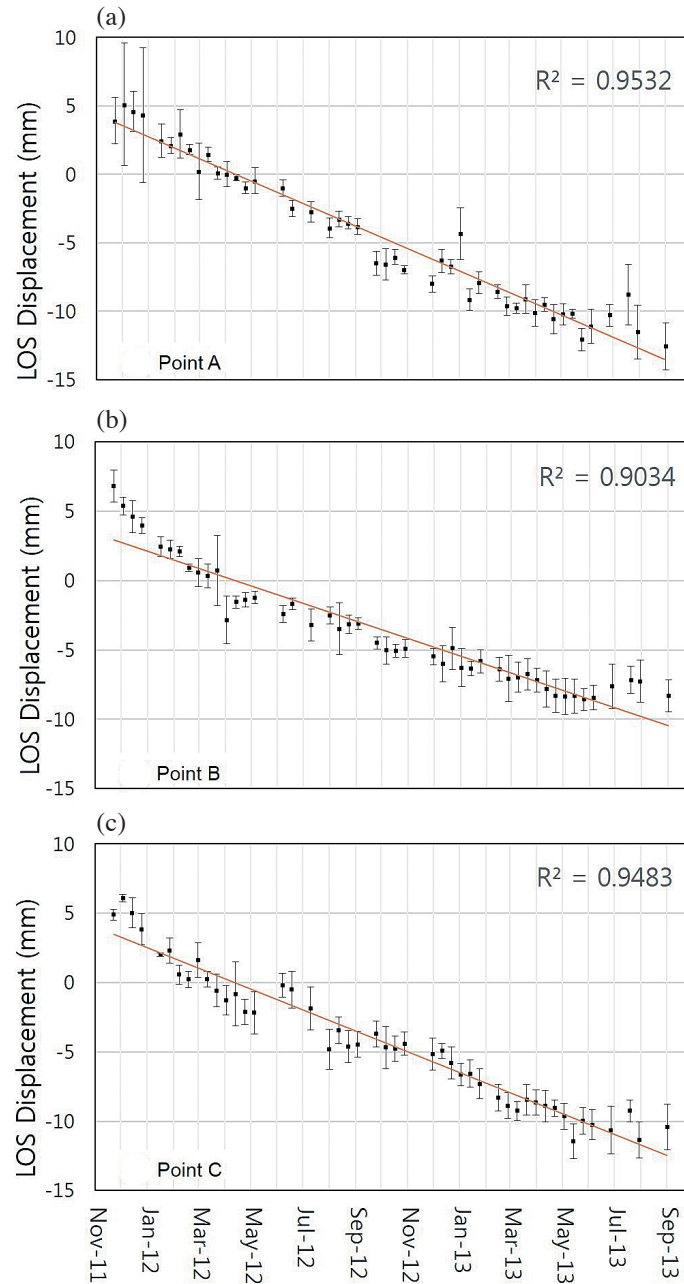
Fig. 6. Time series plot at PSs on "Point A (a)", "Point B (b)" and "Point C (c)" buildings marked in Fig. 5. Dots and bars indicate mean displacement and standard error, respectively. Continuous line indicates best-fit linear model.

was reported in this area in 2015, and this area is very close to the areas where holes were detected in an investigation conducted by Seoul Metropolitan Government in 2014.

GPR exploration for underground cavity monitoring was conducted after a road collapse occurrence. Although it is not possible to directly prove that road collapses occur in relation to subsidence, many road collapses have been reported in major settlement areas detected by TerraSAR-X PS processing. GPR survey of the road collapse site revealed the stratigraphic deflection, and a small settlement was also observed at the ground surface by visual inspection

(Seoul Metropolitan Government 2016).

These results show that the methodology used in this study is an effective way of quantitatively measuring the risk that large buildings in downtown areas will collapse. This risk can be determined in advance. While settlement extensometers, which monitor movements, have been directly installed into buildings with a high risk of collapse, the method used in this study can be used to observe an entire downtown area, and effectively analyze high-risk buildings. Using this method, displacements in downtown areas can be analyzed to a precision of mm/yr, regardless of the time

of day or weather conditions. If the PS method developed in this study is integrated with spatial information, this method can be used as a base technology for monitoring abnormal movements of large buildings in downtown areas.

Despite these benefits, this study has limitations. First, we were unable to conduct on-site investigations or undertake long-term monitoring of the large buildings with high displacement rates. This would be done by installing extensometers in the buildings, but as those buildings are currently used for residential and commercial purposes, we are not able to do this. Thus, the underground hole data released by Seoul Metropolitan Government in 2014 were used and validated as much as possible. Second, it was impossible to monitor the displacement rates of the buildings over a long period as there were limitations in capturing and acquiring TerraSAR-X satellite images. These issues can be addressed by using KOMPSAT-5 satellite images. KOMPSAT-5 is a South Korean SAR satellite, which was launched in August 2013. The results of this study show that we can effectively analyze signs of collapse and settlement in buildings in broad downtown areas. If it is possible to detect and respond to risks of collapse in advance, we can prevent tragedies such as the collapse of and damage to buildings. The method developed in this study can also be used to manage decrepit facilities in downtown areas.

REFERENCES

Adam, N., A. Parizzi, M. Eineder, and M. Crosetto, 2009: Practical persistent scatterer processing validation in the course of the Terrafirma project. *J. Appl. Geophys.*, **69**, 59-65, doi: 10.1016/j.jappgeo.2009.07.002. [Link]

Bakon, M., D. Perissin, M. Lazecky, and J. Papco, 2014: Infrastructure non-linear deformation monitoring via satellite radar interferometry. *Procedia Technology*, **16**, 294-300, doi: 10.1016/j.protcy.2014.10.095. [Link]

Bonano, M., M. Manunta, A. Pepe, L. Paglia, and R. Lanari, 2013: From previous C-band to new X-band SAR systems: Assessment of the DInSAR mapping improvement for deformation time-series retrieval in urban areas. *IEEE Trans. Geosci. Remote Sensing*, **51**, 1973-1984, doi: 10.1109/TGRS.2012.2232933. [Link]

Colesanti, C., A. Ferretti, C. Prati, and F. Rocca, 2003: Monitoring landslides and tectonic motions with the Permanent Scatterers Technique. *Eng. Geol.*, **68**, 3-14, doi: 10.1016/S0013-7952(02)00195-3. [Link]

Crosetto, M., M. Agudo, O. Monserrat, and B. Pucci, 2007: Inter-comparison of persistent scatterer interferometry results. Proceedings of the Fringe 2007 Workshop, 26-30.

Crosetto, M., O. Monserrat, M. Cuevas-González, N. Devanthéry, G. Luzi, and B. Crippa, 2015: Measuring thermal expansion using X-band persistent scatterer interferometry. *ISPRS J. Photogram. Rem. Sens.*, **100**, 84-91, doi: 10.1016/j.isprsjprs.2014.05.006. [Link]

Ferretti, A., C. Prati, and F. Rocca, 2000: Nonlinear subsidence rate estimation using permanent scatterers in differential SAR interferometry. *IEEE Trans. Geosci. Remote Sensing*, **38**, 2202-2212, doi: 10.1109/36.868878. [Link]

Ferretti, A., C. Prati, and F. Rocca, 2001: Permanent scatterers in SAR interferometry. *IEEE Trans. Geosci. Remote Sensing*, **39**, 8-20, doi: 10.1109/36.898661. [Link]

Ferretti, A., G. Savio, R. Barzaghi, A. Borghi, S. Musazzi, F. Novali, C. Prati, and F. Rocca, 2007: Submillimeter accuracy of InSAR time series: Experimental validation. *IEEE Trans. Geosci. Remote Sensing*, **45**, 1142-1153, doi: 10.1109/TGRS.2007.894440. [Link]

Fornaro, G., D. Reale, and S. Verde, 2013: Bridge thermal dilation monitoring with millimeter sensitivity via multidimensional SAR imaging. *IEEE Geosci. Rem. Sens. Lett.*, **10**, 677-681, doi: 10.1109/LGRS.2012.2218214. [Link]

Jung, H. C., S. W. Kim, H. S. Jung, K. D. Min, and J. S. Won, 2007: Satellite observation of coal mining subsidence by persistent scatterer analysis. *Eng. Geol.*, **92**, 1-13, doi: 10.1016/j.enggeo.2007.02.007. [Link]

Karila, K., M. Karjalainen, J. Hyyppä, J. Koskinen, V. Saaranen, and P. Rouhiainen, 2013: A comparison of precise leveling and persistent scatterer SAR interferometry for building subsidence rate measurement. *ISPRS Int. J. Geo-Information*, **2**, 797-816, doi: 10.3390/ijgi2030797. [Link]

KICT (Korea Institute of Civil Engineering and Building Technology), 2015: Evaluation of the Risk of Large Structure Collapse through Analysis of Structure Displacement, KICT. 1-4.

Kim, S. W., S. Wdowinski, T. H. Dixon, F. Amelung, J. W. Kim, and J. S. Won, 2010: Measurements and predictions of subsidence induced by soil consolidation

using persistent scatterer InSAR and a hyperbolic model. *Geophys. Res. Lett.*, **37**, doi: 10.1029/2009GL041644. [Link]

Kim, S. W., S. Wdowinski, F. Amelung, T. H. Dixon, and J. S. Won, 2013: Interferometric coherence analysis of the Everglades Wetlands, South Florida. *IEEE Trans. Geosci. Remote Sensing*, **51**, 5210-5224, doi: 10.1109/TGRS.2012.2231418. [Link]

Massonnet, D. and K. L. Feigl, 1998: Radar interferometry and its application to changes in the earth's surface. *Rev. Geophys.*, **36**, 441-500, doi: 10.1029/97RG03139. [Link]

Merritt, F. S., 1976: Standard Handbook for Civil Engineers, McGraw-Hill, New York, 1321 pp.

Monserrat, O., M. Crosetto, M. Cuevas, and B. Crippa, 2011: The thermal expansion component of Persistent Scatterer Interferometry observations. *IEEE Geosci. Rem. Sens. Lett.*, **8**, 864-868, doi: 10.1109/LGRS.2011.2119463. [Link]

Reale, D., G. Fornaro, A. Pauciullo, X. Zhu, and R. Bamler, 2011: Tomographic imaging and monitoring of buildings with very high resolution SAR data. *IEEE Geosci. Rem. Sens. Lett.*, **8**, 661-665, doi: 10.1109/LGRS.2010.2098845. [Link]

Seoul Metropolitan Government, 2014: Japanese Geological Exploration Company, Seoul Metropolitan Survey Result 41 Sinkhole Detection.

Seoul Metropolitan Government, 2016: 2016 Soeul White Paper, 64-104. Available at http://ebook.seoul.go.kr/Viewer/I09HPEUZ6IYK.

UN (United Nations), 2014: World Urbanization Prospects, UN 7-12.

Wegmuller, U. and C. Werner, 2015: Mitigation of thermal expansion phase in persistent scatterer interferometry in an urban environment. 2015 Joint Urban Remote Sensing Event (JURSE), Lausanne, IEEE, doi: 10.1109/JURSE.2015.7120505. [Link]

Zebker, H. A., P. A. Rosen, R. M. Goldstein, A. Gabriel, and C. L. Werner, 1994: On the derivation of coseismic displacement fields using differential radar interferometry: The Landers earthquake. *J. Geophys. Res.*, **99**, 19617-19634, doi: 10.1029/94jb01179. [Link]